13th Australasian Fluid Mechanics Conference
Monash University, Melbourne, Australia
13-18 December 1998

SIMULATING THE TURBULENT TAYLOR-COUETTE FLOWS USING DNS

J. D. Li

School of the Built Environment, Victoria University of Technology,
P.O. Box 14428, MCMC, Melbourne, 8001, AUSTRALIA

ABSTRACT

Turbulent Taylor-Couette flows between two cylinders with the inner cylinder rotating are simulated using Direct Numerical Simulation (DNS) at high Taylor's number using the finite difference scheme. In this paper, the numerical scheme used is given, and preliminary results on the mean velocity and turbulent quantities are presented. It is found that the mean velocity results are consistent with the experimental ones at the same geometry, the total shear stress profile agrees well with the theoretical prediction. The difference in turbulent intensity magnitude between turbulent Taylor-Couette flows and unidirectional turbulent wall shear flows is explained using the energy equations.

1. INTRODUCTION

Turbulent flow between concentric long cylinders is one of the simplest turbulent shear flows. In this flow, the Reynolds stress equations are all ordinary differential equations. In this aspect, its simplicity is comparable to turbulent flows in pipes or 2-D channels, although our understanding of it is far less than that of the other flows. In comparison with unidirectional turbulent shear flows, centrifugal forces affect the turbulence between the rotating cylinders because the mean streamlines are curved. Modeling of this streamline curvature has long been a difficult task (Hanjalic, 1994).

During the last twenty years, DNS has been used in studying turbulent flows in simple flow geometry, these include turbulent flows in pipes (Eggels, et al., 1994), 2-D channels (Moin & Kim, 1982), and turbulent boundary layers (Spalart, 1988). The geometry in turbulent Taylor-Couette flows is similar to that in pipes where turbulence in both the tangential and axial directions can be assumed to be periodical. To the authors' knowledge, DNS has not been used to study the turbulent Taylor-Couette flows at reasonably high Reynolds numbers.

In this paper, the turbulent Taylor-Couette flows between two concentric cylinders with the inner cylinder rotating are studied using the DNS at T/T_c=1,344. Here T is the Taylor number and T_c is the critical Taylor number. The Naver-Stokes equations are solved directly in the cylindrical coordinate using a second order accurate finite differences scheme. The paper is arranged as follows. In section 2 the numerical scheme and the boundary conditions used are given. In section 3, the mean velocity and turbulent quantities from the simulation are presented. It is found that the mean angular momentum is consistent with that of Taylor (1935), Smith & Townsend (1982) and Li & Wu (1998). The mean velocity is also presented using the inner scaling as suggested by Smith & Townsend (1982), and it is found that viscous sublayers similar to that in the unidirectional turbulent wall shear flows exit. Also a log law can be fitted to the mean velocity defect with constants different from those in the unidirectional wall shear flows. The results for total shear stress and turbulent intensities are presented. It is found that the total shear stress results from the present DNS agree very well with theoretical predictions, and the magnitude of the turbulent intensities are different from those in unidirectional turbulent wall shear flows. This difference is explained using the energy equations. Finally, discussion and conclusions are presented in section 4.

2. NUMERICAL SCHEME, BOUNDARY AND INITIAL CONDITIONS

Figure 1 shows the schematic diagram of the flow geometry in the present DNS study. Here the coordinate

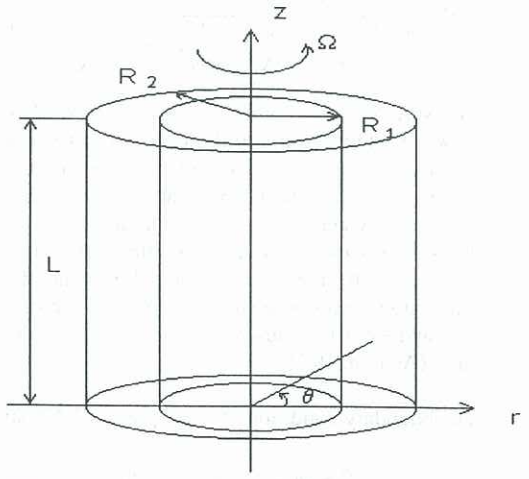

Figure 1 Schematic diagram of the geometry used in simulating the Taylor-Couette flow.

systems are chosen as radius r, tangential θ, and axial z, with the corresponding velocity components v_r, v_θ, and v_z, respectively. The inner and outer radii of the two cylinders are R_1 and R_2, the inner cylinder angular speed is Ω, and the axial length of the simulation is L. The Taylor's number is defined as

$$T = \frac{2(1-\eta)}{(1+\eta)}\mathrm{Re}_d^{\,2}, \qquad \mathrm{Re}_d = \frac{V_1 d}{\nu} \tag{1}$$

Here $\eta=R_1/R_2$, $V_1=R_1\Omega$, $d=R_2-R_1$ and ν is the kinetic viscosity.

The Naver-Stokes equations are discritized as (predictor):

$$\frac{\bar{v}^{*}-\bar{v}^{n-1}}{2\Delta t^{+}} = -[\nabla.\bar{v}\bar{v}]^{n} - \frac{1}{\mathrm{Re}_1}\nabla^2\bar{v}^{n-1} \tag{2}$$

Here v is the velocity vector normalized by V_1, $V_1=R_1\Omega$, $t^+=R_1/V_1$, $\mathrm{Re}_1=V_1R_1/\nu$, and the superscript * is for the intermediate step. In the above equation, Leap-Frog (LF) scheme is used for the time discretization of the convection term, and Euler-Forward scheme is used for the diffusive term. For the spatial discretization, center difference scheme has been used. The correction step is,

$$\frac{\bar{v}^{n+1} - \bar{v}^{*}}{2\Delta t^{+}} = -\nabla \pi \tag{3}$$

where π is the pressure fluctuations, and satisfies the Poisson equation

$$\nabla^2\pi = \frac{1}{2\Delta t^{+}}\nabla\bar{v}^{*} \tag{4}$$

Here the velocity vectors at the time step n+1 satisfy the continuity equation

$$\nabla\bar{v}^{n+1} = 0. \tag{5}$$

In the simulation, explicit scheme has been used, and Δt^+ is estimated from

$$\Delta t^{+} = \frac{0.5}{\frac{|v_r|}{\Delta r}+\frac{|v_\theta|}{r\Delta\theta}+\frac{|v_z|}{\Delta z}+\frac{4}{\mathrm{Re}_1}\left(\frac{1}{\Delta r^2}+\frac{1}{r^2\Delta\theta^2}+\frac{1}{\Delta z^2}\right)} \tag{6}$$

to ensure stability (Pourquie, 1994). Unlike DNS for pipe flows, in the present turbulent Taylor-Couette flows, $r_{min}=R_1$ and thus no singularity exist as that in the pipe center where singularity exists at $r_{min}=0$. Because of this, no implicit scheme is needed as that in pipe flows (Eggls, 1994). To avoid de-coupling of the odd and even time levels due to the use of the LF-scheme during the simulation, every time step a weak coupling between the odd and even time levels is made by using the Asselin filter (Asselin, 1972).

The boundary conditions for the present DNS simulation are

$$\begin{aligned}\phi(r,\theta+2\pi,z,t) &= \phi(r,\theta,z,t)\\ \phi(r,\theta,z+L,t) &= \phi(r,\theta,z,t)\end{aligned} \tag{7}$$

in the θ- and z-directions, where ϕ is any velocity component or pressure. In the radial r-direction,

$$\begin{aligned}&v_r(R_1,\theta,z,t) = v_r(R_2,\theta,z,t) = 0\\ &v_z(R_1,\theta,z,t) = v_z(R_2,\theta,z,t) = 0\\ &v_\theta(R_1,\theta,z,t) = V_1, \qquad v_\theta(R_2,\theta,z,t) = 0\end{aligned} \tag{8}$$

In using the explicit scheme, the pressure boundary conditions in the radial direction needs only to be specified at one point on the outer cylinder surface. The initial conditions are the laminar mean velocity V with disturbances generated from a random number generator. The simulation was carried out for more than 100 non-dimensional eddy-turn-over time $t^+=tV_1/R_1$, and it was found that by this time the steady state of the turbulent velocity field was achieved.

In performing DNS, uniform staggered grids for the θ- and z-directions and logarithmic grid for the r direction within the gap between the two cylinders, with the small grid size near the inner cylinder, were used. Such a non-uniform grid in the radial direction is based on the finding that the smallest turbulent length scale increases with r in the turbulent Taylor-Couette flows (Li & Wu, 1998). The number of grid points used were 64×128×256 for the r, θ- and z-directions, respectively. The Poisson equation was solved by means of an algorithm based on the Fast Fourier Transform (FFT). The maximum imbalance within each control volume for the continuity equation was monitored, and was in general less than 10^{-18}. The simulation was performed using a Pentium II computer with 256 Mb RAM. In general, the time required for each time step was about 45 second, and less than a week's time was needed for 10,000 time steps.

3. RESULTS

One of the requirements for DNS to give credible results is to ensure that the spatial and temporal resolutions must be sufficiently fine to capture even the smallest scales of turbulent motions. Also the normal-to-the-wall grid distribution must be able to resolve the steep gradients in the velocity field near the wall from which follows that the normal-to-the-wall grid spacing must be the same order of magnitude as the viscous length scale ν/V_τ, where V_τ, is the wall shear velocity. Unlike that in the unidirectional pipe flows, there is no available relationship between the wall shear velocity and the Reynolds number in the literature (Li & Wu, 1998), especially at low Reynolds number. Because of this, a trial and error process has been adopted to determine the maximum Reynolds number that the current computer used can give sufficient resolution. It is found that, with $R_2=2R_1$, the maximum Reynolds number based on R_1 that can be simulated is about 2500. This gives $T=4.2\times10^6$ and $T/T_c=1{,}344$ with T_c estimated from Roberts (1965). According to Barcilon & Brindley (1984), the state of the flow at such Taylor number should be steady state turbulence.

In turbulent pipe flows, the length L in the axial direction is normally taken to be sufficiently long to ensure that the turbulent motions at the two ends of the pipe do not correlate with each other. In Eggle et al (1994), L=5D, where D is the diameter of the pipe. In the present simulation, $L=12R_1$ was used. It is found that with such an axial length, the correlation of the turbulent motions at the two ends of the cylinder is very small (<0.05). The mean grid width estimated from

$$\Delta^{+} = (r^{+}\Delta r^{+}\Delta\theta^{+}\Delta z^{+})^{1/3} \tag{9}$$

is about 5. This is very close to the value used in Eggle. (1994).

The time step Δt^+ estimated from (6) was about $0.007t^+$ when the flows approach steady state. The convective time scale $\Delta t \sim \nu/v^2 = 0.08t^+$, and this is an order of magnitude larger than that used in the present simulation. Also it can be estimated that the Kolmogrov time scale is much larger than the convective time scale. Thus the time step used in the present simulation is small enough to resolve the smallest turbulent time scale. This also supports the suggestions of Verstappen & Veldman (1997) which state that, in DNS, the time resolution from the stability criteria is the most critical one.

Figure 2 shows the normalized mean angular momentum rV/R_1V_1 from the present DNS simulation. The results shown in figure 2 are similar to that of Smith & Townsend (1982) and Li & Wu (1998) at the similar flow geometry, i.e. the mean angular momentum decreases from its value at the inner cylinder surface to about half of that within a small viscous layer. Over a large proportion of the gap width between the two cylinders, the angular momentum varies only slightly, indicating the mean velocity there is close to that for potential flow. Near the outer cylinder surface, the angular momentum decreases again rapidly to zero within a viscous sublayer.

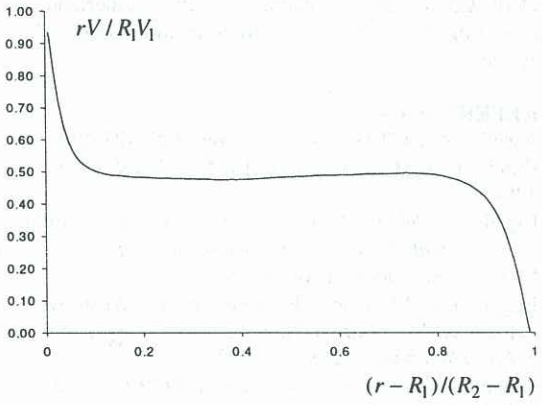

Figure 2 Normalized mean angular momentum.

Figure 3 shows the mean velocity profile using the inner scaling following the suggestion of Smith & Townsend (1982), i.e. velocity is normalized by the wall shear velocity V_τ and the local distance from the inner cylinder surface is normalized by the viscous length scale ν/V_τ. It can be seen from figure 3 that, near the wall, the velocity profile follows the linear relationship, same as that in unidirectional wall shear flows. Away from the wall, a log law of the form

$$\frac{V_1 - V}{V_\tau} = \frac{1}{\kappa}(\ln(y^+) + A) \qquad (10)$$

with A=3.3 and k=0.8 fits the data up to y+=100. Here $y+=(r-R_1)V_\tau/\nu$. These constants are different from those given by Smith & Townsend (1982). They found that k=0.41 and A=1.8, which are close to those for unidirectional turbulent wall shear flows. Li & Wu

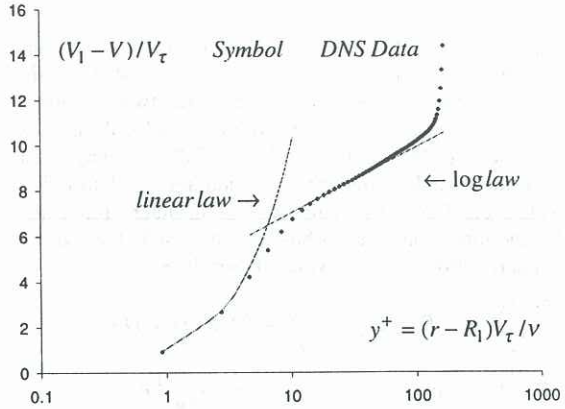

Figure 3 Mean velocity profile under inner scaling.

(1998) found A=5.1 and k=0.8. Further work is needed to determine these constants.

Figure 4 shows the total shear stress profiles from the simulation at one instant. Theoretically, it can be shown that

$$\tau = \frac{\rho V_\tau^2}{(r/R_1)^2} = \rho[\overline{v_r' v_\theta'} - \nu r \frac{\partial}{\partial r}(\frac{V}{r})] \qquad (11)$$

where the first term on the r.h.s. of (11) is the Reynolds shear stress and the second is the contribution from the viscosity. In figure 4, the above theoretical relationship is also shown. It can be seen from the figure that the predicted total shear stress profile agrees very well with the theoretical one. Equ. (11) also shows that the viscous length scale ν/V_τ at the outer cylinder surface is R_2/R_1 times that of near the inner cylinder surface. In the present case, this shows that the thickness of the viscous sublayer at the outer cylinder is twice that near the inner cylinder surface. Because of this, the requirement for spatial resolution near the outer cylinder surface would not be as fine as that near the inner cylinder surface. This justifies the non-uniform grid size used in the radial direction, with smaller grid size near the inner cylinder surface.

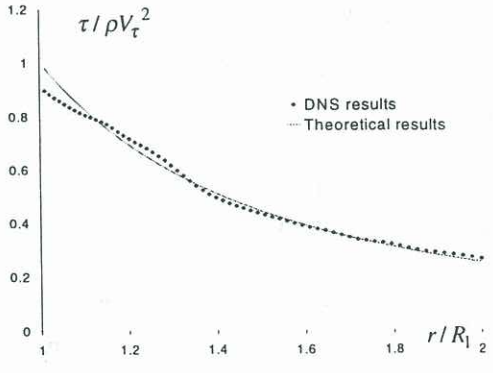

Figure 4 Normalized total shear stress.

Figure 5 shows the turbulent intensities from the current simulation. It can be seen from the figure that, in the central region of the gap between the two cylinders, $v_r'>v_z'>v_\theta'$. This is consistent with the results of Smith & Townsend (1982) and Li & Wu (1998). In comparison with the turbulent intensities in unidirectional turbulent wall shear flows, the magnitude of turbulent intensities for the three components has been reversed. This can be explained from the following relationships

$$\begin{aligned}
\frac{\partial \overline{v_r'v_r'}}{\partial t} &= TD + 4\overline{v_r'v_\theta'}\frac{V_\theta}{r} + VP + VD + DS \\
\frac{\partial \overline{v_\theta'v_\theta'}}{\partial t} &= TD - 2\overline{v_r'v_\theta'}\frac{\partial V_\theta}{\partial r} - 2\overline{v_r'v_\theta'}\frac{V_\theta}{r} \\
&\quad + VP + VD + DS \\
\frac{\partial \overline{v_z'v_z'}}{\partial t} &= TD + VP + VD + DS
\end{aligned} \tag{12}$$

where TD is the turbulent diffusion, VP the velocity-pressure gradient interaction, VD viscous diffusion and DS is the viscous dissipation. In (12), only the production and convective transport terms are explicitly given, the others terms are similar to those for unidirectional turbulent wall shear flows. Equ. (12) shows that there is a strong production term in the equation for $v_r'v_r'$ from the centrifugal force. The transport equation for $v_z'v_z'$ is the same as that in the unidirectional turbulent shear flows, which shows that the energy for the axial velocity component comes from TD, VP and VD. In the equation for $v_\theta'v_\theta'$, there is a production term from the Reynolds shear stress, same as that in unidirectional shear flows, but there is also a convective transport term which destroys the v_θ fluctuations. Because the tangential velocity decays slightly slower than the inverse power law (figure 3), and from (11) it can be shown that the net effect from the production and convective transport terms in the transport equation for $v'_\theta v'_\theta$ results in a destruction. This explains why $v_r'>v_z'>v'_\theta$ in the turbulent Taylor-Couette flows in comparison with $v_r'<v_z'<v'_\theta$ in unidirectional turbulent wall shear flows.

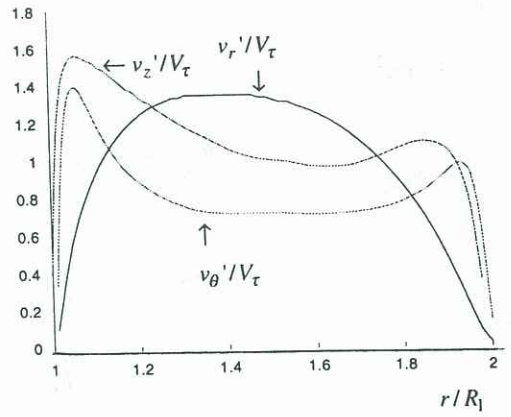

Figure 5 Profiles of turbulent intensities.

4. DISCUSSION AND CONCLUSIONS

DNS has been used to simulate the turbulent Taylor-Couette flows at high Taylor's number, and preliminary results have been presented. It is found that the results for the mean velocity and turbulent intensities are consistent with the experimental results of Smith & Townsend (1982) and Li & Wu (1998). Near the cylinder surface, the mean velocity defect follows a linear relationship, same as that in unidirectional turbulent wall shear flows. Outside the sublayer, the mean velocity defect follows a log law with different constants from those in unidirectional wall shear flows. The total shear stress profiles from the simulation agree well with the theoretical predictions and shows that the thickness of the viscous sublayers near the two cylinder surfaces should be linearly proportional to the radius ratio. For the Turbulent Taylor-Couette flow, in the central region between the two cylinders, the magnitude of the turbulent intensities is such that the intensity for the radial direction is the largest and that in the tangential direction is the smallest. This has been explained using the energy equations.

ACKNOWLEDGEMENT

The author would like to thank Professor Nieuwstadt of Delft University of Technology, the Netherlands, for providing their DNS code in a cylindrical coordinate system.

REFERENCES

Asselin, R. 1972 *Mon. Weather Rev.* **100**, 487-490.

Barcilon, A. & Brindley, J. 1984 *J. Fluid Mech.*, **143**, 429-449.

Eggels, J.G.M. 1994 *Direct and Large Eddy Simulation of Turbulent Flows in a Cylindrical Pipe Geometry,* Ph.D. Thesis, Delft University Press.

Eggels, J. G. M., Unger, F., Weiss, M. H., Westerweel, J., Adrian, R. J., Friedrich, R. & Nieuwstadt, F. T. M. 1994 *J. Fluid Mechanics,* **268**, 175-209.

Hanjalic, K. 1994 *Int. J. heat and Fluid Flow,* **15**, *No.3*, 178-203.

Li, J.D. & Wu., J.1998 *Submitted for publication.*

Moin, P. & Kim, J. 1982 *J. Fluid Mech.* **118,** 341-377.

Roberts, P.H. 1965 ***Proc. R. Soc. Lond.*** A**283**, 531.

Pourquie, M. J. B. M. 1994 *Large-eddy simulation of a free turbulent jet.* Ph.D. thesis, Delft University of Technology, The Netherlands.

Spalart, P. R. 1988 *J. Fluid Mech.* **187,** 61-98.

Smith, G. P. & Townsend, A. A. 1982 *J. Fluid Mech.* **123**, 187-217.

Taylor, G. I. 1936 *Proc. R. Soc. Lond.* A**157**, 546.

Verstappen, R.W.C.P. & Veldman, A.E.P. 1997 *J. Eng. Math.*